AZD115 - Inductive Sensing Application Note

Inductive sensing application note for Azoteq's ProxFusion® devices

Contents

1 Overview

As the need for more robust contactless sensing increases, inductive sensing is increasingly gaining momentum as a favourable sensing technology. The contactless nature of inductive sensing allows for robust designs that can withstand harsh environmental conditions while maintaining predictable results and performance. Azoteq's ProxFusion® series of devices offers cutting-edge, low-cost, low-power inductive sensing solutions that can be used in various applications, from simple buttons to rotational encoders.

This application note looks into the principal operation of inductive sensing and provides insight into the various design parameters that should be considered for inductive sensing applications. These parameters for consideration include coil shape and size, LC tank resonant frequency, LC tank quality factor, and metal target properties.

2 Introduction to inductive sensing

Inductive sensing detects the change in inductance of an inductor as a conducting metal object or target is brought within proximity of the inductor. The sensing inductor is usually made up of a winding wire or a spiral PCB track. The change in inductance of the sensor is dependent on the sensor-target distance, as well as the composition and size of the target.

When an AC signal is applied to the sensing coil, a time-varying electromagnetic (EM) field is generated around the coil. When a conducting metal target is brought into proximity to the coil, the time-varying EM field around the coil induces eddy currents in the target, as shown in Figure 2.1.

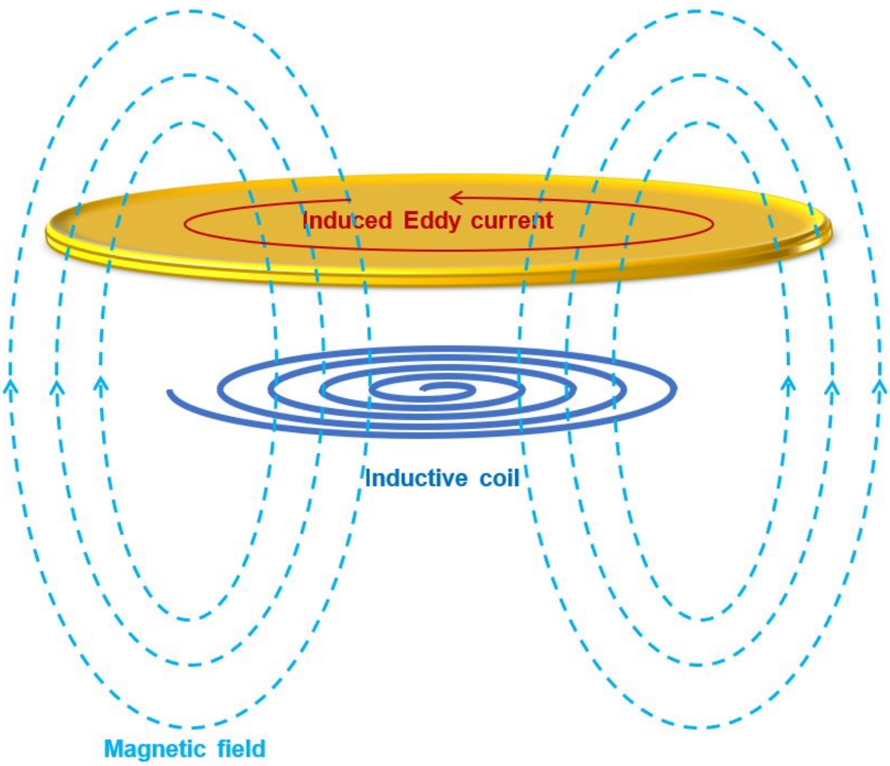

Figure 2.1: Induced eddy currents on a metal target

The direction of the induced eddy currents in the target is such that it generates an opposing EM field, which reduces the overall inductance of the sensing coil. This change in inductance caused by the metal target on the sensing coil is measured by the ProxFusion® devices on a CRx pin.

3 Inductive sensor

3.1 Inductor types

Inductors are available in different shapes and sizes, and the choice of inductor used as a sensor depends on the intended application. Described below are some of the more commonly available off-the-shelf inductors and their typical inductive sensing applications.

3.1.1 Air core inductors

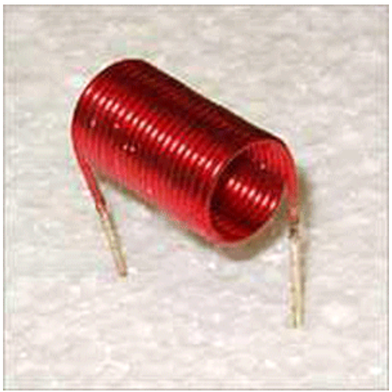

Figure 3.1: Air core inductor

- Typically have low inductance values due to the low permeability of the air core.
- Ideal for sensing applications with limited PCB space.
- Lead extensions enable the designer to place the inductor closer to the target, allowing for the use of inductors with small diameters.
- Targets with a small cross-sectional area and long length can be reliably detected when passing through the coil centre.

3.1.2 Ferrite core inductors

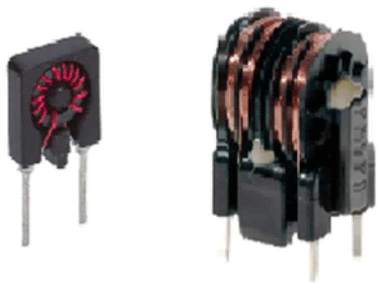

Figure 3.2: Ferrite core inductor

- Typically have higher inductance values due to the high permeability of the ferrite core.
- Stray magnetic fields from strong magnets can influence the inductance of the coil.
- The sensing applications are similar to that of the air core inductors.

3.1.3 Toroidal core inductors

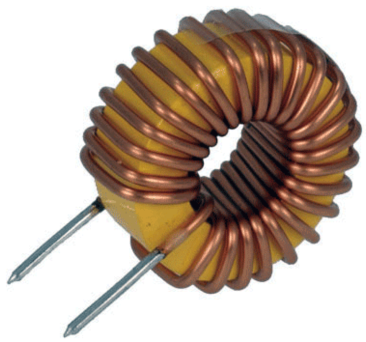

Figure 3.3: Toroidal core inductor

- Typically have higher inductance values due to the high permeability of the ferrite core.
- Stray magnetic fields from strong magnets can influence the inductance of the coil.
- The donut shape ferrite core contains the magnetic field.
- The sensing range of coils is severely limited due to the contained magnetic field.

3.1.4 Axial inductors

Figure 3.4: Axial inductors

- Typically have higher inductance values due to the high permeability of the ferrite core.
- Limited sensing range due to the small cross-sectional area of windings.

3.1.5 Shielded surface mount inductors

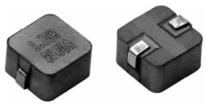

Figure 3.5: Shielded surface mount inductors

- Magnetic fields from the inductor coil windings are shielded by the outer cover.
- Since there is limited to no interaction of the magnetic fields with the metal target, the shielded coils should not be used for inductive sensing.

3.1.6 Wireless charging coils

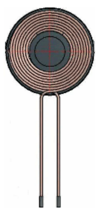

Figure 3.6: Wireless charging coils

- Ferrite material is placed behind the coil to increase the inductance, provide shielding, and focus the magnetic fields.
- Coil windings consist of multi-stranded wire to reduce losses from skin effects.
- These coils are well suited for inductive sensing applications.

3.1.7 Multi-layer chip inductors

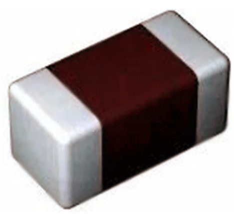

Figure 3.7: Multi-layer chip inductor

- The coil pattern is printed in layers to create an SMD inductor.
- The core of the inductor can either be ferrite or ceramic.
- Ceramic core inductors are preferred since they are less susceptible to stray external magnetic fields.
- A small form factor makes these inductors ideal for applications with limited PCBA space.
- Due to the small coil winding diameter, the range of the magnetic field is also small.
- The metal target needs to be placed very close to the coil, usually a few hundred micrometres, for inductive sensing applications.

3.1.8 PCB coils

Figure 3.8: PCB coils

- A spiral coil pattern is printed on a FR4-PCB or FPC.
- The physical shape and size of the coil can be designed to meet a wide range of inductive sensing applications.
- The cost of design is reduced since coils are printed on existing PCBs.
- A ferrite sheet can be placed behind the coil for shielding and increased inductance.

For most inductive sensing applications, PCB coils are recommended, as they provide the best balance between cost and performance.

3.2 PCB coils

3.2.1 Coil shape

Common shapes used for PCB coils include circular, square, hexagonal, and octagonal. The coil shape defines the size and geometry of the magnetic field. Circular coils generate a symmetrical circular magnetic field, which is preferable for sensing a metal target that is moving perpendicular to the PCB coil plane. Square coils will also generate a symmetrical magnetic field but will have the added advantage of a larger inductance value compared to a circular coil of similar outer diameter. Hexagonal and octagonal coils can be used to approximate a circular coil while requiring a smaller PCB footprint.

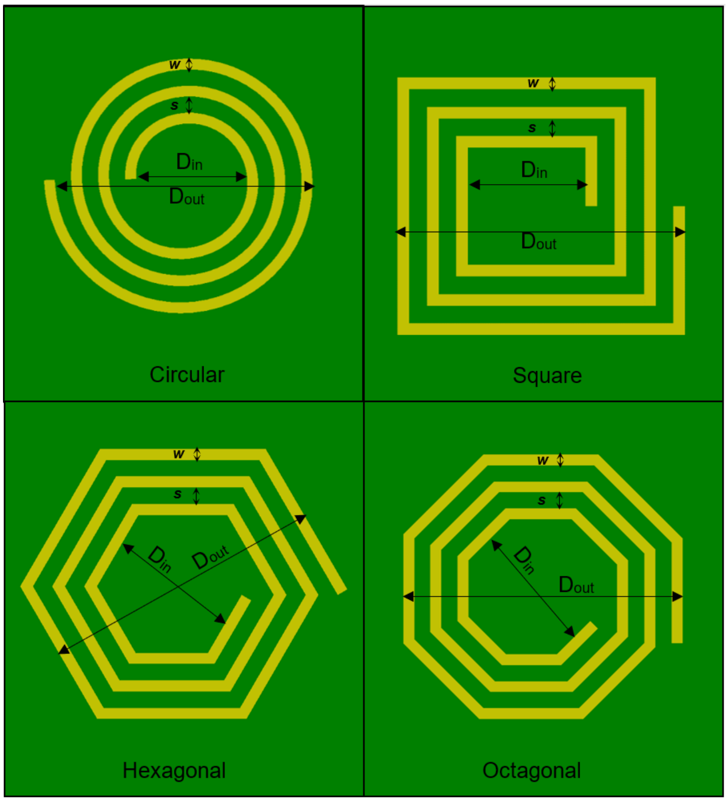

Figure 3.9: Spiral coil shapes

The choice of coil shape is mainly influenced by the sensing application and the available PCB space for coil routing.

3.2.2 Inductance of PCB coils

The inductance value (L_s) for a single layer planar PCB coil [1] can be approximated as:

$$L_s = \frac{\mu_o n^2 d_{avg} c_1}{2}\left(\ln\left(\frac{c_2}{\rho}\right) + c_3\rho + c_4\rho^2\right), \tag{1}$$

where

- μ_o is the permeability of free space, $4\pi \times 10^{-7}$ H/m,
- n is the number of turns in the coil,

- d_{avg} is the average diameter, calculated as:

$$d_{avg} = 0.5(d_{out} + d_{in}), \tag{2}$$

- d_{out} is the coil outer diameter,
- d_{in} is the coil inner diameter,
- ρ is the fill ratio, defined as:

$$\rho = (d_{out} - d_{in})/(d_{out} + d_{in}), \tag{3}$$

- c_1, c_2, c_3 and c_4 are geometric dependent coefficients given in Table 3.1.

Table 3.1: Planar coil coefficients for inductance expression

Geometry	c_1	c_2	c_3	c_4
Square	1.27	2.07	0.18	0.13
Hexagonal	1.09	2.23	0.00	0.17
Octagonal	1.07	2.29	0.00	0.19
Circle	1.00	2.46	0.00	0.20

3.2.3 Multi-layer coils

The inductance of a PCB coil can be increased by connecting multiple coils on different layers of the PCB in series. To ensure that the magnetic fields of the current flowing in the different layers do not cancel each other out, the winding direction of the coils is reversed from one layer to the next, as shown in Figure 3.10.

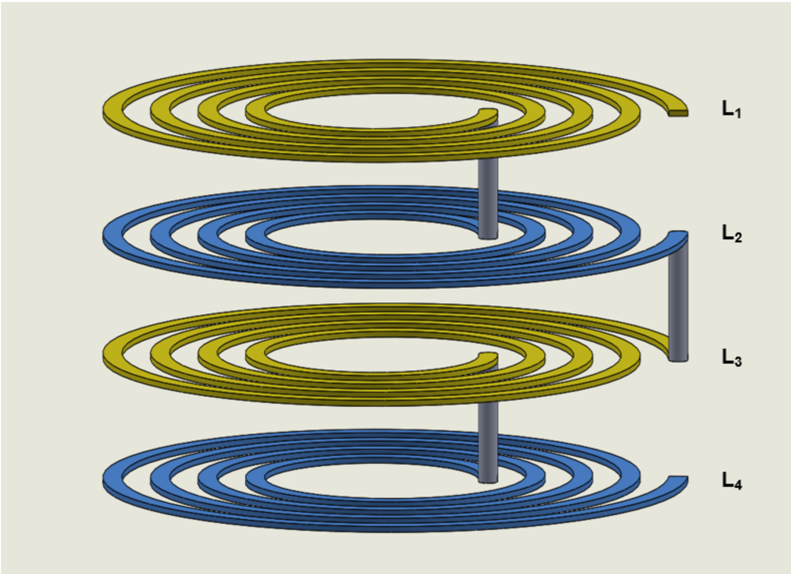

Figure 3.10: Multi-layer spiral coil

The inductance of a two layer inductor coil can be approximated using Equation (4) [2]. The inductance of the coil on the first layer L_1 and second layer L_2 are calculated using Equation (1). The mutual inductance M between the two coils is related to the coupling factor, K_C, as given in Equation (5) and Equation (6):

$$L_{Total} = L_1 + L_2 \pm 2M \tag{4}$$

$$M = K_C \sqrt{L_1 \times L_2} \tag{5}$$

$$K_C = \frac{n^2}{(0.184 \cdot x^3 - 0.525 \cdot x^2 + 1.038 \cdot x + 1.001) \times (1.67n^2 - 5.84n + 65) \times 0.64} \tag{6}$$

where

- x is the distance between the two coil layers in mm
- n is the number of coil turns in a given layer

For a coil with more than 2 layers, there are more than 2 coupling factors that need to be calculated. The 4 layered coil in Figure 3.10 has 6 coupling factors in total, $K_{C_{12}}$, $K_{C_{13}}$, $K_{C_{14}}$, $K_{C_{23}}$, $K_{C_{24}}$, and $K_{C_{34}}$, where $K_{C_{ij}}$ is the coupling factor between different coil layers i and j. The total inductance of the 4 layered coil is given by:

$$L_{total} = L_1 + L_2 + L_3 + L_4 + 2 \cdot (K_{C_{12}} + K_{C_{13}} + K_{C_{14}} + K_{C_{23}} + K_{C_{24}} + K_{C_{34}}) \cdot \sqrt{L_1 L_2} \tag{7}$$

Since the coils on each layer have the same geometric shape, the 4 layer coil inductance can be expressed as follows:

$$L_{total} = 4L_s + 2 \cdot (K_{C_{12}} + K_{C_{13}} + K_{C_{14}} + K_{C_{23}} + K_{C_{24}} + K_{C_{34}}) \cdot L_s \tag{8}$$

3.2.4 Inductor losses

When an AC current flows through a conductor, the current flow tends to be concentrated on the surface of the conductor due to the skin effect. The current density decreases as you move away from the surface of the conductor, towards the centre of the conductor. This effectively reduces the cross-sectional area available for the current to flow. The skin effect introduces resistive losses R_s as a result of the reduced cross-sectional area. For a given AC signal with frequency f, the skin depth δ is defined as the point at which the current density of the conductor reaches approximately 37% of its value at the surface of the conductor.

$$\delta = \sqrt{\frac{\rho}{\mu_0 \cdot \mu_r \cdot f \cdot \pi}} \tag{9}$$

$$R_s = \frac{l \cdot \rho}{w \cdot \delta\left(1 - \exp\left(-\frac{t}{\delta}\right)\right)} \tag{10}$$

where:

- l is the coil length of coil in meters
- ρ is resistivity of copper trace in Ohm-meter
- μ_0 permeability of free space = $4 \cdot \pi \times 10^{-7} \frac{H}{m}$
- μ_r relative permeability of copper trace = 1
- f is the AC signal Tx frequency in Hertz
- w trace width in meters

- t trace thickness in meters

PCB coils for inductive sensing should be designed to minimise AC losses since a larger R_s decreases the coil current, resulting in a weaker magnetic field strength. High sensor Q values also require minimal R_s (see section 4.4). The coil losses can be minimised as follows:

- minimizing coil length by:
  - optimizing the number of turns (see section 3.2.5)
  - using multiple layers to increase coil inductance instead of a long single-layer coil
- increasing trace height
- increasing trace width
- increasing the skin depth by lowering the frequency of the signal current through the coil

3.2.5 Number of turns

From Equation (1), the inductance of a coil is directly proportional to the number of coil turns. However, as n increases, d_{in} decreases, which in turn decreases d_{avg}. This means that as n increases, the change in inductance decreases, while the length and consequently the AC losses of the coil increase.

The outer coil turns contribute more to the coil inductance than the inner coil turns. The optimum number of turns is when $d_{in}/d_{out} \geq 0.30$, as this point retains the majority of the inductance while limiting AC losses and maintaining a high Q value.

3.2.6 Coil physical size and sensing range

For coil shapes with equal dimensions, such as circular and square coils, the perpendicular sensing range h is determined by the outer diameter D_{out} of the coils. As a general a rule of thumb, a coil with an outer diameter of D_{out} will have an effective sensing range of up to half D_{out}. For coil shapes with unequal dimensions, such as rectangular coils, D_{out} is defined by the smallest dimension of the coil. The inductance value has no influence on the sensing range of the coil.

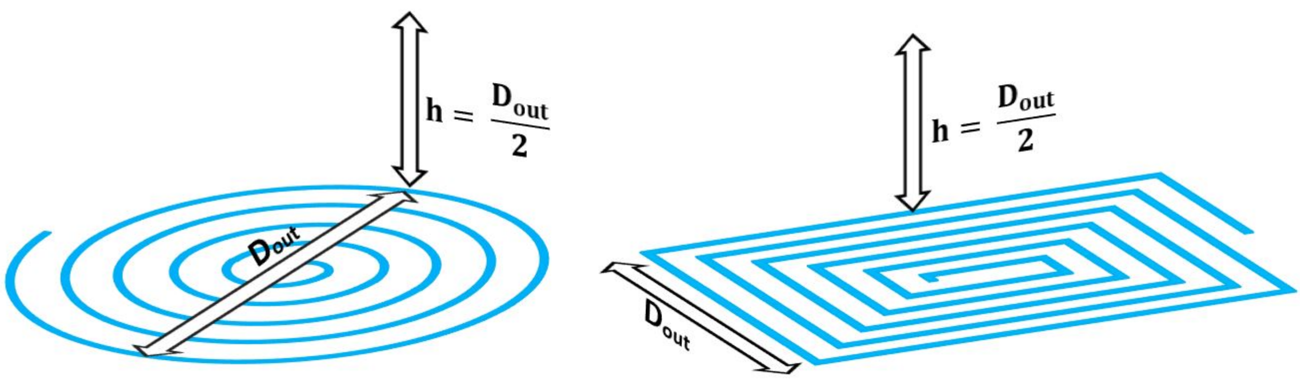

Figure 3.11: Sensing range based on coil outer diameter

3.2.7 Parasitic capacitance and self-resonant frequency

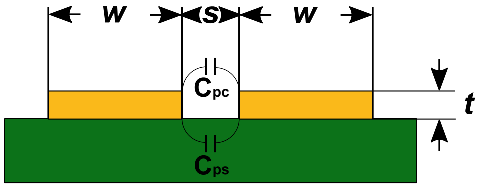

Figure 3.12: Adjacent trace parallel plate capacitance

A cross-sectional view of a PCB spiral coil shows a parallel plate parasitic capacitance C_p between the sidewalls of the conductors. This parallel capacitance is distributed along the length of the spiral coil gap and is influenced by the air and the FR4 dielectric substrate.

$$C_p = C_{pc} + C_{ps} \approx (\alpha \cdot \epsilon_{rc} + \beta \cdot \epsilon_{rs})\epsilon_0 \frac{t}{s} \cdot l_g \tag{11}$$

where

- C_{pc} is the distributed capacitance due to air
- C_{ps} is the distributed capacitance due to FR4 substrate
- ϵ_{rc} is the relative dielectric constant of air $= 1$
- ϵ_{rs} is the relative dielectric constant of FR4 substrate $= 4.4$
- ϵ_0 is the free space permittivity
- s is the coil trace width spacing
- t is the trace thickness
- l_g is the length of the coil gap
- $(\alpha = 0.90, \beta = 0.1)$ for air and FR4 respectively

As the signal frequency increases, the EM fields find it easier to propagate through the parasitic capacitance than along the coil windings. The self-resonant frequency (SFR) of the coil is the frequency at which the impedance of the inductor and parasitic capacitance are equal. It is recommended to always operate at frequencies far below the SFR since the parasitic capacitance is not stable at the SFR. In most cases, frequencies less than 60% of the SFR should be used for inductive sensing applications.

4 LC tank circuit

4.1 Resonant frequency

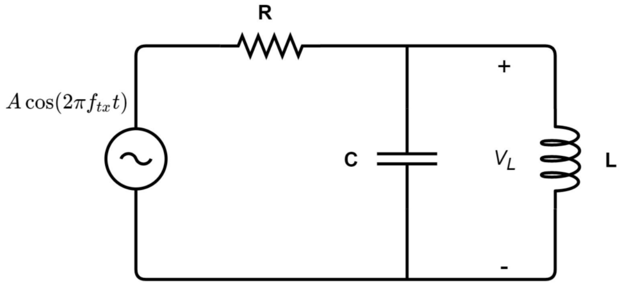

Figure 4.1: LC tank resonant circuit

A suitable inductive sensing magnetic field can be generated using the parallel LC tank resonant circuit in Figure 4.1. The resonant frequency of the tank circuit f_{res} can be approximated using Equation (12).

$$f_{res} = \frac{1}{2\pi\sqrt{LC}}. \tag{12}$$

Figure 4.2 shows the response of the LC tank voltage V_L as the excitation frequency f_{tx} is swept from 1 MHz to 10 MHz. This particular tank circuit is tuned to resonate at 4 MHz, and V_L has the maximum amplitude at this frequency. At the resonant frequency, the impedance of the LC tank circuit is at its maximum. Due to this high impedance, less current is required to generate the EM field, which is crucial for low-power applications.

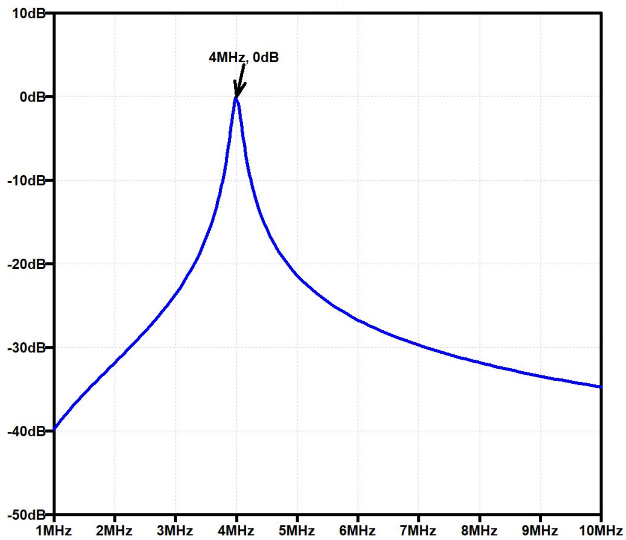

Figure 4.2: Response with 4 MHz resonant frequency

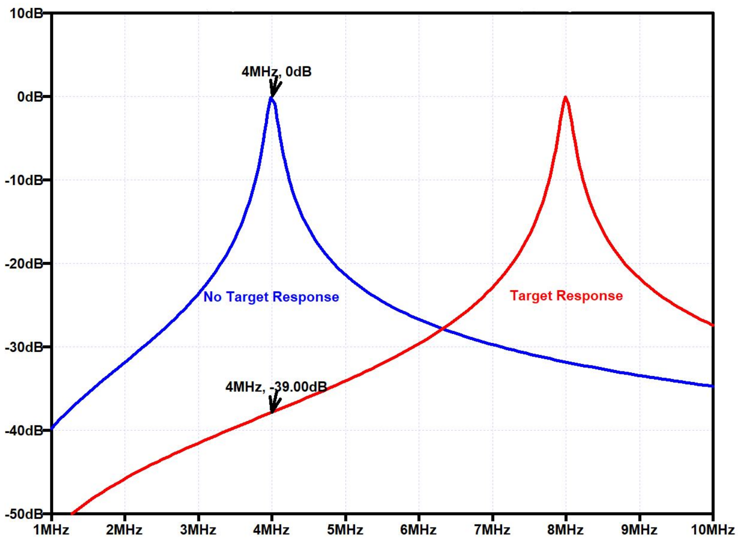

Figure 4.3: LC tank Response with metal target

A metal target interacting with the magnetic field decreases the inductance, and from Equation (12), the decreasing L increases f_{res}. This will translate the band-pass response of the tank circuit to higher frequencies, as shown in Figure 4.3. Since the excitation frequency f_{tx} is fixed, the tank voltage V_L is attenuated by 39 dB. Azoteq ProxFusion® devices generate the excitation signal of frequency f_{tx} on a CTx pin and measure the change in inductance on a CRx pin.

4.2 LC tank parallel impedance

The resonant frequency of the LC tank is the point where the impedance of the capacitor is equal to that of the inductor. At this frequency, the impedance of the LC tank is at its maximum and approaches infinity, assuming ideal L and C components. In practice, the inductor model has a series resistor representing the distributed AC losses, as mentioned in Section 3.2.4. These losses draw current from the tank circuit and limit the tank impedance R_p to a finite value.

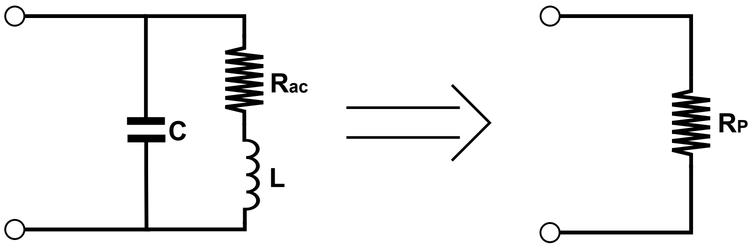

Figure 4.4: Practical inductor model and tank equivalent impedance

Equation (13) approximates the finite LC tank impedance and shows that as R_{ac} increases, R_p decreases. Azoteq ProxFusion® devices require a minimum tank impedance R_{p_min} of $0.8\,\mathrm{k\Omega}$ for optimal operation. PCB coil design must aim to minimise R_{ac} and achieve an LC tank impedance of at least R_{p_min}.

$$R_p = \frac{L}{CR_{ac}} \tag{13}$$

4.3 Measuring resonant frequency and impedance

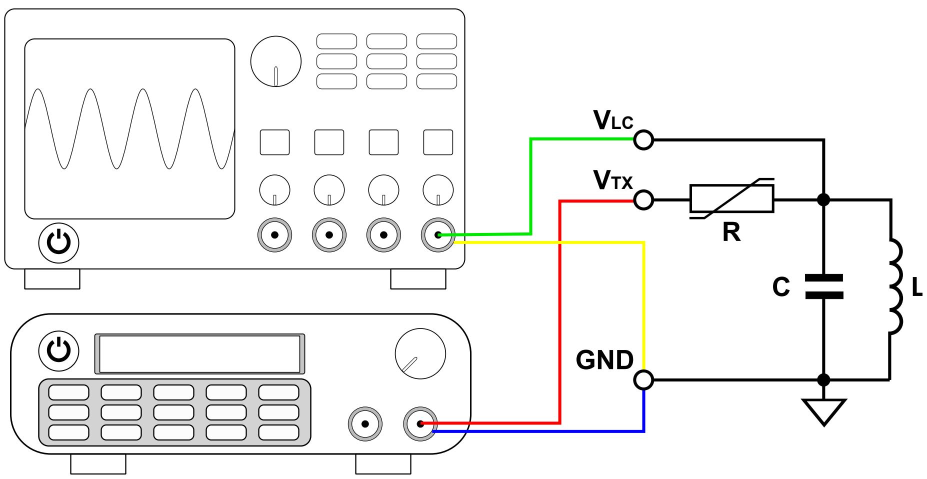

Figure 4.5: Rp measurement setup. Top: Oscilloscope. Bottom: Signal generator

Using the setup in the figure above, the resonant frequency and impedance of the LC tank can be measured. The signal generator provides a frequency-swept signal (V_{TX}) and is connected to the LC tank through the variable-series resistor R. The voltage across the LC tank (V_{LC}) is measured on the oscilloscope. The time domain view of the oscilloscope will show an increase in amplitude V_{LC} as the sweep frequency gets closer to f_{res} and a decrease in V_{LC} as the sweep frequency moves away from f_{res}.

Series resistor R is adjusted as follows:

- If there is little to no signal measured on the oscilloscope, the series resistance R should be decreased until the observed maximum amplitude of $V_{LC} = V_{TX}/2$.
- If the maximum measured amplitude of V_{LC} is larger than $V_{TX}/2$, the series resistance R should be increased until the observed maximum amplitude of $V_{LC} = V_{TX}/2$.

Resonant frequency f_{res} is measured as follows:

- Switch oscilloscope measuring mode to the frequency domain[i].
- Set the oscilloscope display persist to infinity[ii].
- Allow the frequency sweep from the signal generator to complete a couple of sweeps.
- Use the oscilloscope cursors[iii] to measure f_{res}, which is the frequency at the maximum amplitude.

Impedance of the LC tank R_p is measured as follows:

- Exit sweep mode on the signal generator and set the waveform to a sine wave with a frequency of f_{res} and amplitude V_{TX}[iv] of choice.
- Adjust series resistor R until $V_{LC} = V_{TX}/2$.
- The impedance R_p is equal to the adjusted resistor value R.

4.4 LC tank quality factor

The quality factor of the LC tank circuit is defined as the ratio between the energy stored, and the energy dissipated due to losses in the tank circuit. A major component of these losses is the distributed AC losses along the length of the coil windings, as mentioned in section 3.2.4. The LC tank circuit can be modelled using series or parallel equivalent impedance circuits, as shown in Figure 4.6. The series resistor R_s represents the inductor AC losses R_{ac}.

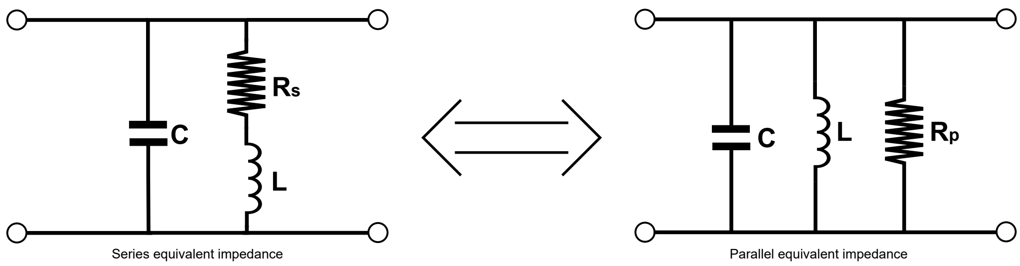

Figure 4.6: LC tank series and parallel impedance model

The parallel equivalent impedance R_p can be approximated as:

$$R_p = \frac{(2\pi f L)^2}{R_s} \tag{14}$$

The Q value expressions for the series and parallel equivalent circuits are given in Equation (15) and Equation (16) respectively. Since the circuits are equivalent, the Q values for both circuits are also

[i] Tektronix TDS2014B : Math Menu → Operation → FFT
[ii] Tektronix TDS2014B : Display → Persist → Infinity
[iii] Tektronix TDS2014B : Cursors → Source → Math; Cursors → Type → Frequency
[iv] A peak to peak of 5V is recommended for most applications

the same.

$$Q_{series} = \frac{2\pi f L}{R_s} \tag{15}$$

$$Q_{parallel} = \frac{R_p}{2\pi f L} \tag{16}$$

$$Q_{series} = Q = Q_{parallel} \tag{17}$$

The 3dB bandwidth of the LC tank circuit at the resonant frequency f_{res} is inversely proportional to the Q value, according to Equation (18). The higher the Q value, the narrower the 3dB bandwidth. For most inductive sensing applications, a high Q value is required; as such, it is recommended to design for minimum inductor AC losses of R_s.

$$BW = \frac{2\pi f_{res}}{Q} \tag{18}$$

From Figure 4.7, as the Q value increases, the bandwidth of the LC tank decreases and improves the sensitivity for inductive sensing.

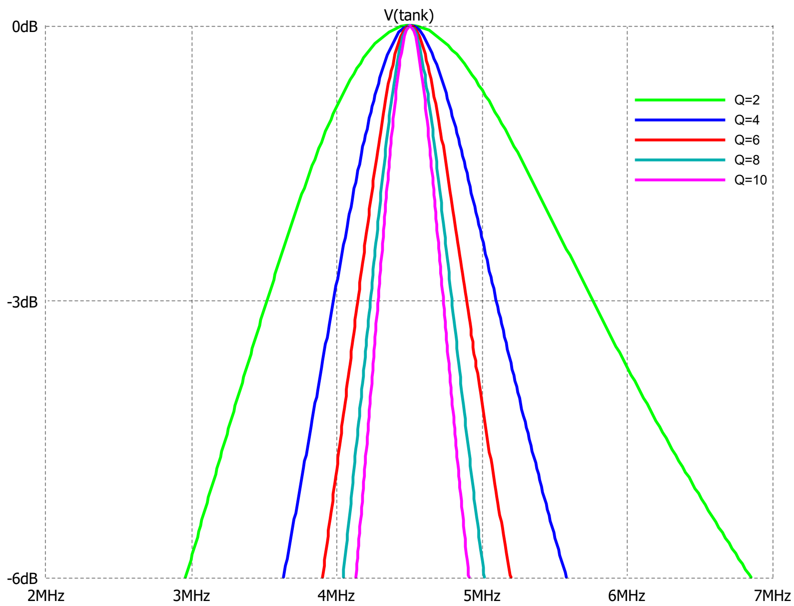

Figure 4.7: LC tank bandwidth for given Q values

4.5 Tank capacitor selection

The choice of capacitor influences the characteristics of the tank circuit. The ideal capacitor has minimal parasitic resistance and maintains capacitance stability under operational conditions. For inductive sensing applications, the C0G/NP0 capacitors are preferred as they provide the following characteristics:

- Available in small packages over a wide range of capacitance values.

- Good capacitance stability over a wide temperature range.
- Low ESR compared to the Rs of the inductor; therefore, the inductor Rs dominates the Q and 3dB bandwidth of the LC tank.
- Minimal signal distortion.
- High operating frequencies with typically higher SFR values compared to the inductor coil.
- Minimum capacitance change due to voltage change across the capacitor ($\frac{dC}{dV}$).
- No piezoelectric shifts in capacitance value due to physical stress.
- Minimum capacitance shifts with ageing.
- Non-polarized capacitance.

4.6 Metal target

4.6.1 Detection methods

Inductive sensing can detect the movement of a metal target along the axis normal to the plane of the coil (axial detection) or along a plane parallel to it (lateral detection).

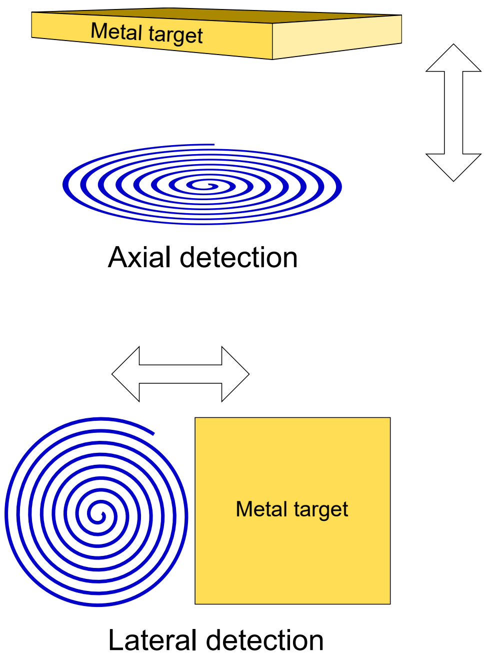

Figure 4.8: Axial and lateral detection

4.6.2 Image Eddy currents and target shape

The Eddy currents generated by the interaction of the metal target with the AC magnetic field will follow a closed-loop path of least-resistance. This path can be represented by a mirror image of the coil current.

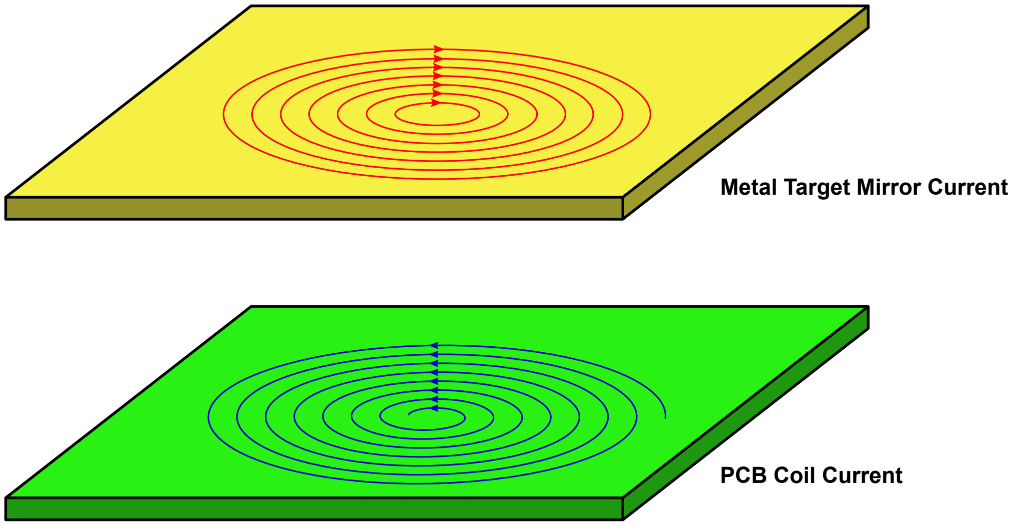

Figure 4.9: Induced closed loop mirror image currents

Any gaps, voids, or discontinuities in the shape of the target will cause the eddy currents to navigate around these obstacles and not follow the mirror image path of least-resistance. This results in eddy current losses that weaken the opposing field coupling between the coil and target, resulting in a reduced inductance change.

4.6.3 Skin depth

Eddy currents are generated on the surface of the target conductor due to of the skin effect. The skin depth represents the distance from the conductor surface at which the current reduces by $1/e$ and represents the depth containing 63.2% of the current.

Table 4.1: Skin depth current of conductor

Skin depth δ	Percentage of total current
1	63.2
2	86.5
3	95.0
4	98.2
5	99.3

It is recommended to have at least 2 skin depths of current flowing through the target metal conductor and this is achieved by:

- Increasing the TX frequency.
- Selecting target material with higher conductivity.
- Increasing the thickness of the metal target.

4.6.4 Target composition

The higher the electrical conductivity of the target, the higher the induced Eddy currents and strength of the opposing magnetic field. This increases the change in sensor inductance and improves the measurement resolution. Rigid materials that do not warp or bend are preferred as they provided more accurate and repeatable results. Below is a comparison of some common materials that can be used as the metal target:

- Copper
  - Very good electrical conductivity, 5.96×10^7 S/m.
  - Heavier and less rigid compared to Aluminium.
  - Mechanically rigid targets can be implemented using copper pour on PCB.
- Aluminium
  - Good electrical conductivity, but less than copper, 3.50×10^7 S/m.
  - Light weight compared to copper and stainless steel.
  - Mechanically rigid.
- Steel
  - Very low electrical conductivity, 0.145×10^7 S/m.
  - Different alloys have different magnetic properties:
    - Martensitic alloys are magnetic.
    - Austenitic alloys are non-magnetic.
  - Magnetic steel alloys increase coil inductance at lower frequencies due to the high permeability of the alloys. The magnetic field lines permeate the alloy and do not generate Eddy currents.
  - Frequencies higher than 2MHz should be used for magnetic steel targets, where the skin depth is small enough to generate surface eddy currents that block the magnetic fields from permeating the magnetic alloy.
- Conductive inks
  - Typically have very low conductivity.
  - Inks have to be sprayed on rigid surfaces such as hard plastic to form rigid targets.

A Appendix

A.1 Tx frequency options

Table A.1: FOSC = 14MHz frequency options

Period Register	Tx Frequency
0	7.00 MHz
1	3.50 MHz
2	2.30 MHz
3	1.75 MHz
4	1.40 MHz
5	1.16 MHz
6	1.00 MHz
7	875 kHz
8	777 kHz
9	700 kHz
10	636 kHz
11	583 kHz
12	538 kHz
13	500 kHz

Note: Tx frequency option of 14MHz is configurable and independent of the period register. Refer to specific device datasheet.

Table A.2: FOSC = 18MHz frequency options

Period Register	Tx Frequency
0	9.00 MHz
1	4.50 MHz
2	3.00 MHz
3	2.25 MHz
4	1.80 MHz
5	1.50 MHz
6	1.28 MHz
7	1.12 MHz
8	1.00 MHz
9	900 kHz
10	818 kHz
11	750 kHz
12	692 kHz
13	642 kHz
14	600 kHz
15	562 kHz
16	529 kHz
17	500 kHz

Note: Tx frequency option of 18MHz is configurable and independent of the period register. Refer to specific device datasheet.

A.2 ProxFusion® inductive application circuit

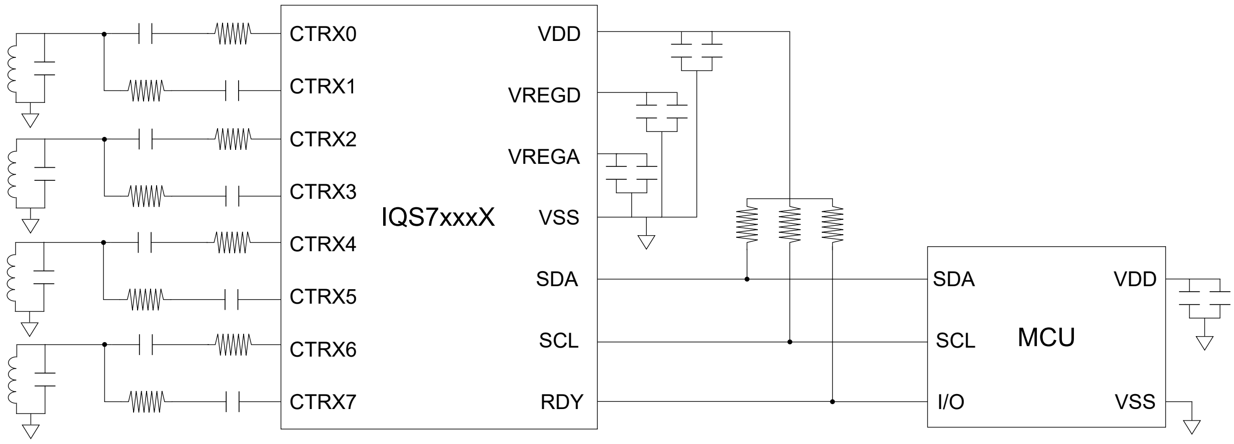

Figure A.1: IQS7xxxX inductive application circuit

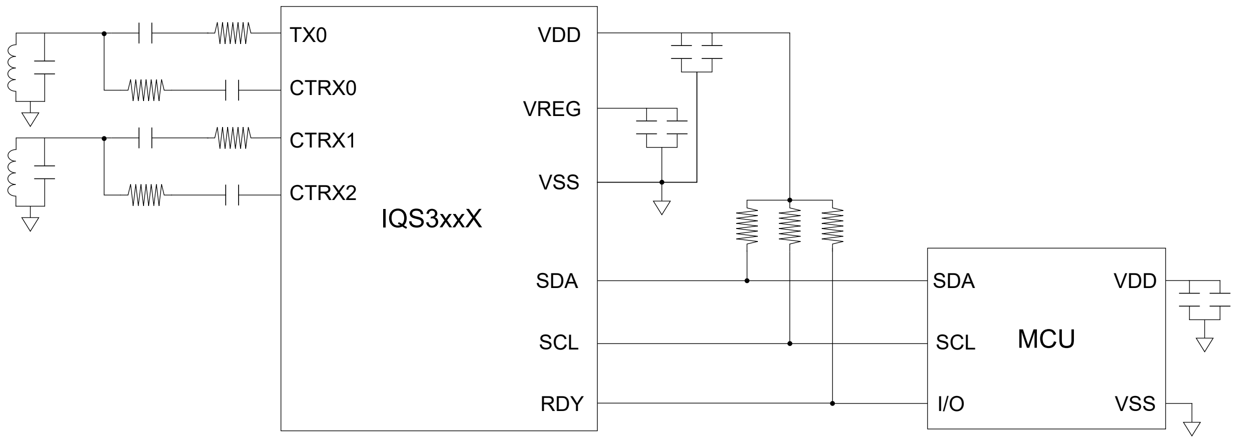

Figure A.2: IQS3xxX inductive application circuit

B Revision History

Release	Date	Changes
v1.0	March 2020	Initial release
v1.1	October 2022	Inductive sensing device schematic update
		Additional design details
v1.2	January 2023	Additional design details

References

[1] S. S. Mohan, M. del Mar Hershenson, S. P. Boyd, and T. H. Lee, “Simple accurate expressions for planar spiral inductances,” *IEEE Journal of solid-state circuits*, vol. 34, no. 10, pp. 1419–1424, 1999.

[2] J. Zhao, “A new calculation for designing multilayer planar spiral inductors,” *EDN (Electrical Design News)*, vol. 55, no. 14, p. 37, 2010.

Contact Information

	USA	Asia	South Africa
Physical Address	11940 Jollyville Suite 120-S Austin TX 78759 USA	Room 501A, Block A T-Share International Centre Taoyuan Road, Nanshan District Shenzhen, Guangdong, PRC	1 Bergsig Avenue Paarl 7646 South Africa
Postal Address	11940 Jollyville Suite 120-S Austin TX 78759 USA	Room 501A, Block A T-Share International Centre Taoyuan Road, Nanshan District Shenzhen, Guangdong, PRC	PO Box 3534 Paarl 7620 South Africa
Tel	+1 512 538 1995	+86 755 8303 5294 ext 808	+27 21 863 0033
Email	info@azoteq.com	info@azoteq.com	info@azoteq.com

Visit www.azoteq.com
for a list of distributors and worldwide representation.